Hindawi
Advances in Civil Engineering
Volume 2022, Article ID 8058525, 17 pages
https://doi.org/10.1155/2022/8058525

Research Article

Numerical Analysis of the Mechanical Responses and Transition Section Design of Pavement Structures in the Entrance and Exit Sections of Highway Tunnel

Xueying Zhao,[1] **Aiqin Shen**,[2] **and Baofu Ma**[3]

[1]*School of Civil Engineering, Qingdao University of Technology, Qingdao 266520, China*
[2]*Key Laboratory of Highway Engineering in Special Region of Ministry of Education, Chang'an University, Xi'an 710064, China*
[3]*China Communications Construction Company Highway Consultants Co., Ltd.,, Beijing, China*

Correspondence should be addressed to Xueying Zhao; zhaoxueying@qut.edu.cn

Received 25 April 2022; Revised 16 August 2022; Accepted 6 September 2022; Published 3 October 2022

Academic Editor: Elisabete Teixeira

The entrance and exit sections of a tunnel are subject to different environments, pavements, and traffic conditions, which is quite different from the average highway, and it should be considered differentially, when designing pavement structures. However, there are no clear regulations on it in Chinese specifications. Over the years, a lot of studies were carried on the entrance and exit sections of a tunnel, but there are few ones on the pavement design and its mechanical response characteristics. In this paper, the Huangjiayu tunnel and the Yangkou tunnel in Shandong province were taken as case study engineerings and their pavement structures in the entrance and exit sections are referred to as Str-1 and Str-2, respectively. In Str-1, asphalt pavement was applied inside and outside the tunnel and a transition section was applied. In Str-2, asphalt pavement was applied outside the tunnel and concrete pavement was applied inside the tunnel when it was built in 2004 and a transition section was not applied. Meanwhile, 7 alternative pavement structures (referred to as Str-1a~Str-1g), in which the lengths of transition sections were different, were proposed, simulated, and analyzed through FE program ANSYS. Through the analysis of maximum shear stresses in asphalt courses and tensile stresses at the bottom of base courses, it was found that setting a transition structure is essential, and it can ensure the continuity of pavements and significantly reduce the sudden change of shear stress of asphalt layer and thus prevent premature pavement distresses. Hence, Str-1 is more reasonable compared with Str-2. Besides, it was also found that when the asphalt surface outside the tunnel is designed to be three layers, it is more appropriate to use Str-1, in which the concrete slab in the transition structure has variable cross section, and the length of the concrete slab is 4.5 m. When the asphalt surface outside the tunnel is designed to be two layers, Str-1b is more reasonable and the length of the concrete slab is also 4.5 m.

1. Introduction

With the development of the economy and society, tunnels are more and more widely used in China's roads. According to statistics published by the Ministry of Transport of China, the number of highway tunnels in China has exceeded 20000, reaching 21316, and the total length has exceeded 20 million meters, reaching 21.999 million meters at the end of 2020. The entrance and exit sections of a tunnel are the transition parts. It is subject to different environments, pavements, and traffic conditions inside and outside the tunnel, which is quite different from the average highway in all aspects. Due to the semiclosed characteristics of tunnels, vehicles would obviously decelerate and accelerate in the process of driving towards and away from tunnels, which may cause pushing effects on the pavement structures. Moreover, according to the traffic survey, at present, the phenomenon of overloading is still serious. When the vehicle loads increase, the number of equivalent axle loads increases exponentially instead of proportionally, which will cause a serious burden on the pavement. Hence, the entrance and exit sections should be considered differentially, when designing the pavement structures.

At present, scholars have carried out a lot of research on the entrance and exit sections of tunnels, which can be mainly divided into the following categories: pavement temperature fields [1–3], linear setting [4–7], brightness design [8–13], and operation safety [14–18]. Despite these studies, there are few ones on the mechanical response characteristics of the pavement structures in these sections. Traditionally, concrete pavement is used inside the tunnel and asphalt pavement is used outside the tunnel in China, due to many reasons, such as the need for fire prevention. Hence, the concrete pavement inside the tunnel is directly connected with the asphalt pavement outside the tunnel. However, under the application of traffic loads, the shear stress at the junction of the two structures exceeds 28.37% of the asphalt pavement in the average section [19], which is very prone to shear failure. Meanwhile, distress investigation shows that such pavement structure design, that is, "concrete pavement inside tunnels + asphalt pavement outside tunnels," will cause frequent cracks in the entrance and exit sections after being used for a short period of time, which will be described in detail in Part 3. In this case, in recent years, there is a trend that asphalt pavement is also applied inside tunnels and a transition structure is set in the middle of pavements inside and outside the tunnel. However, due to the lack of mechanical response analysis, the design of the transition structure is usually based on experience and lack of mechanical guidance. Besides, due to the short paving time, relevant distresses investigation of the transition pavement structure is insufficient, whether it could avoid distresses is still not clear.

Therefore, to guide the pavement design in tunnel entrance and exit sections, it is of vital importance to study the mechanical response of the pavement structure specifically in these sections. In this paper, the Yangkou tunnel of Qingdao Binhai Highway and the Huangjiayu tunnel of Qingdao-Lanzhou Highway in Shandong province were taken as case study engineering. Meanwhile, 7 other alternative pavement structures were selected and their mechanical responses were simulated and analyzed through the FE program (ANSYS). The flowchart of this paper is shown in Figure 1.

This paper is organized as follows:

(1) Analysis of working conditions inside and outside the tunnels, which have great differences and effects on the behavior of the pavement structures

(2) Investigation into the pavement distresses in the tunnel entrance and exit sections

(3) Proposed FE models and mechanical boundary conditions for pavements

(4) Mechanical responses of the pavement structures in entrance and exit sections of the Yangkou Tunnel and the Huangjiayu Tunnel subjected to traffic loads

(5) Proposed 7 alternative pavement structures and their mechanical responses subjected to traffic loads

(6) Conclusions and suggestions for the future pavement design for the tunnel entrance and exit sections

2. Analysis of Working Conditions inside and outside the Tunnels

There are great differences in working conditions inside and outside the tunnels, including environmental conditions (temperature, ventilation, and lighting), pavement structure (structural foundation and width transition), and traffic conditions (frequent braking and channelization). In this part, different pavement structure and traffic conditions will be analyzed specifically since this paper mainly discusses the mechanical response of the tunnel entrance and exit sections under the application of traffic loads. Environmental conditions will be discussed in another paper.

2.1. Pavement Structure

2.1.1. Pavement Foundation inside and outside the Tunnels. The pavement structures inside and outside the tunnels have obvious differences. For the pavement outside a tunnel, the pavement structure is built on the subgrade and its resilience modulus is usually 40~70 MPa. However, for the pavement inside a tunnel, whether invert is set or not, the base course is usually plain concrete, and the whole pavement structure is paved on the bedrock, so that the strength of the bearing layer is much higher than that of the pavement structure outside the tunnel.

If the transition part of the pavement structures inside and outside the tunnel cannot be designed well, a huge stress concentration will be generated at the junction of the two pavement structures, which will seriously affect the service life and reduce the driving quality.

2.1.2. Pavement Width. Highway outside the tunnel is usually two-way traffic, and the cross section is composed of central separation belt, carriageway, hard shoulder, and earth shoulder, while the highway inside the tunnel is one-way traffic, and the cross section is narrowed due to the lack of earth shoulder, shown in Figure 2. Therefore, the transition design of tunnel pavement width is also an important part of the design of tunnel entrance and exit transition section.

2.2. Traffic Conditions

2.2.1. Frequent Acceleration and Deceleration. The design speed outside a tunnel is usually 80~120 km/h, while that inside a tunnel is only 60~80 km/h. The design speed of some special tunnels is even as low as 40 km/h. The difference of design speed makes the driver slow down when entering the tunnel and accelerate when leaving the tunnel. In addition, the "black hole," "black frame," "white hole," and "white frame" effects produced by visual shock led to the need for drivers to slow down when driving near the portal to ensure driving safety. Therefore, acceleration and deceleration in these sections are quite serious.

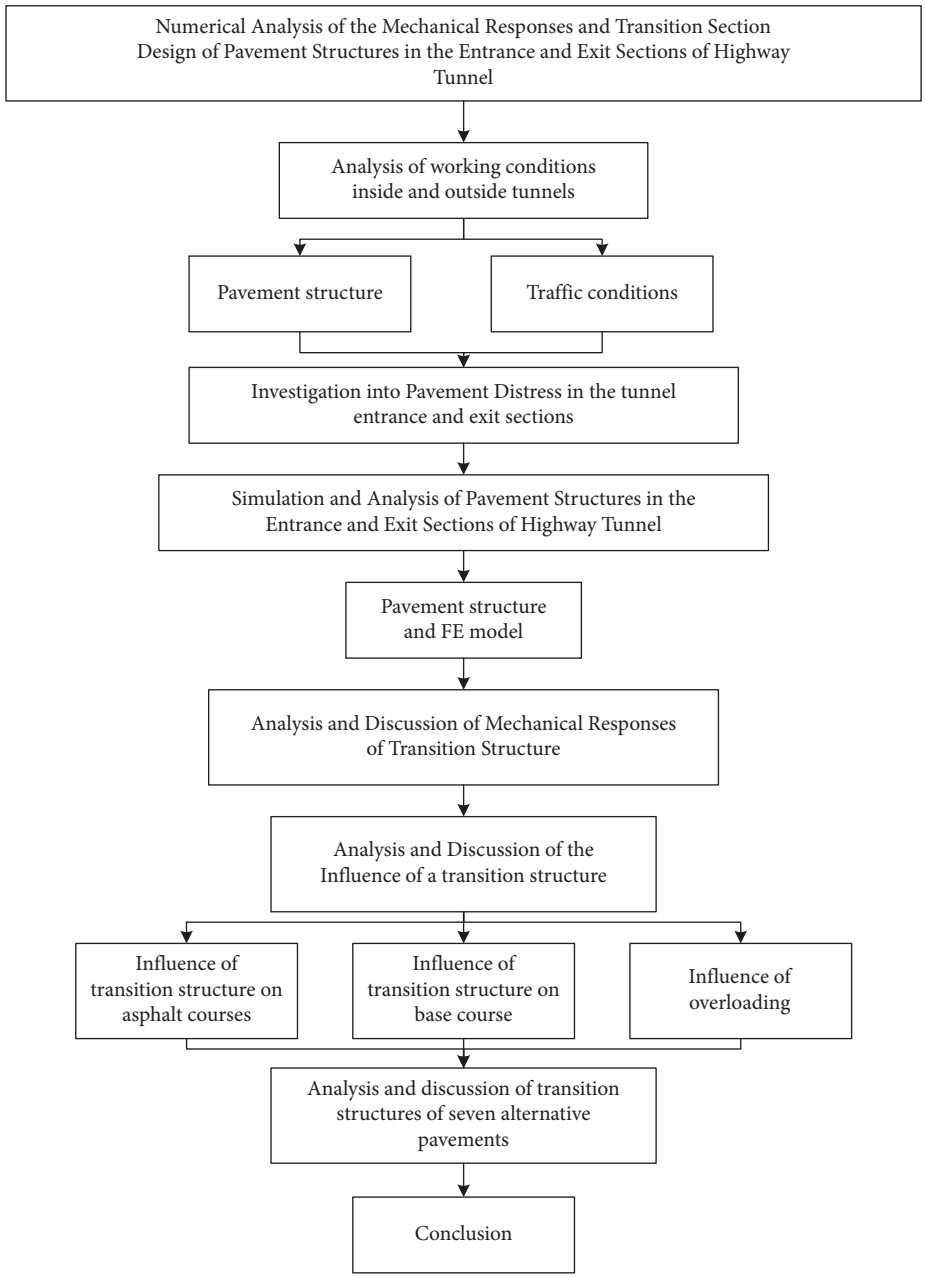

Figure 1: Flowchart of this paper.

2.2.2. Traffic Channelization inside Tunnels. The tunnel is a semiclosed structure, and the wall rock on both sides will seriously affect drivers, so that they will unconsciously drive close to the marking line in the middle of the road after entering the tunnel, which is easy to cause traffic channelization. In addition, for safety reasons, overtaking is not allowed in a tunnel, which makes vehicles often drive from the entrance to the exit in a certain line, further aggravating the channelization phenomenon.

3. Investigation into Pavement Distress in the Tunnel Entrance and Exit Sections

As the connection part, the entrance and exit sections have experienced great differences in the pavement structures and traffic conditions. Distresses often occur in the early stage of service. In this part, distresses in the entrance and exit sections of the Yangkou tunnel of Qingdao Binhai Highway are investigated.

Yangkou tunnel is the first long tunnel in Jiaodong Peninsula, and its position is shown in Figure 3. It was opened to traffic at the end of 2006. After several years of use, the pavement surface performance has been declining. The distresses in the sections of tunnel entrance and exit since it was open were investigated, and results are shown in Table 1 and the detection lane areas are shown in Figure 4.

Concrete pavement was applied inside the Yangkou tunnel and asphalt pavement was applied outside the tunnel when it was first designed in 2004. It can be seen from Table 1 that the skid resistance of the pavement in the entrance and

Figure 2: The narrowed cross section.

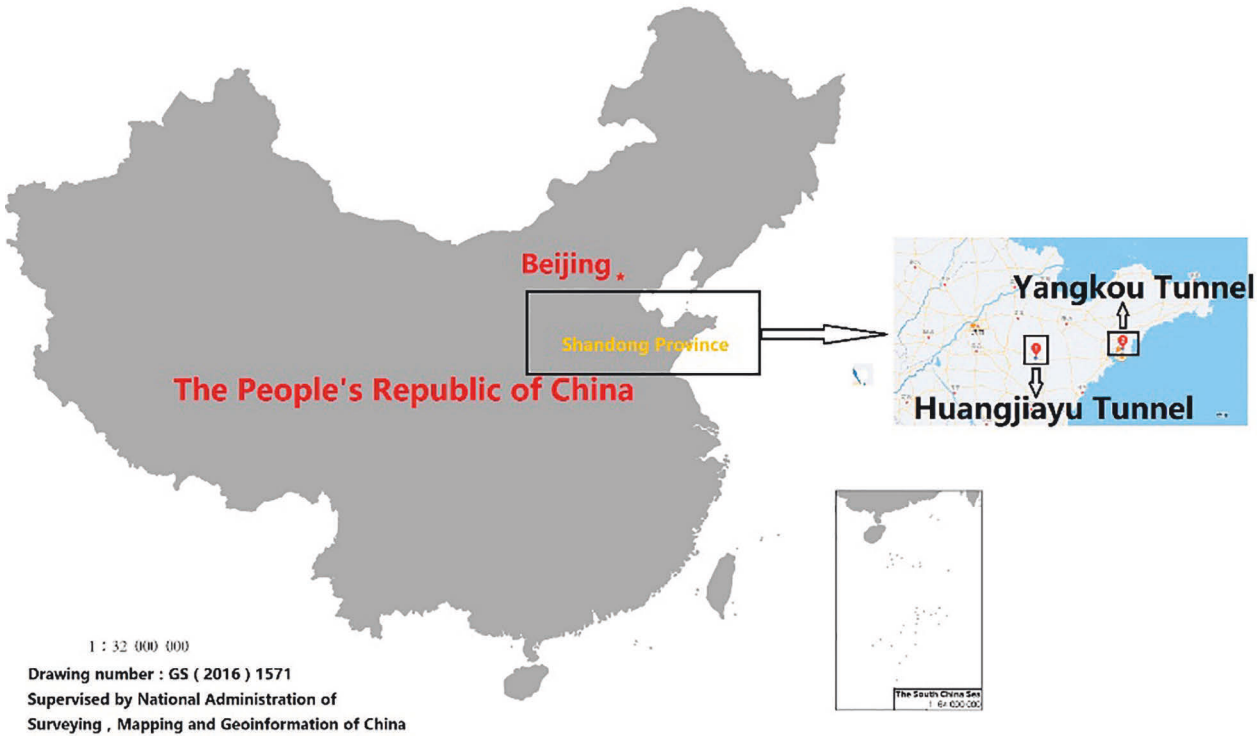

Figure 3: Location of Yangkou tunnel and Huangjiayu tunnel [20].

exit sections decreases continuously in the process of use. According to a large number of studies on tunnel traffic accidents [21, 22], the decrease of pavement adhesion coefficient is an important reason of traffic accidents near the tunnel entrance and exit sections. In addition, there are also a small number of cracks and pits in the pavement in these sections. Cracks including transverse cracks and longitudinal cracks (shown in Figure 5, red lines) are mainly concentrated in the surface layer and hardly develop into the base course.

Therefore, in August 2013, the Yangkou tunnel was rehabilitated and the picture after rehabilitation is shown in Figure 6. The original concrete pavement inside tunnel was milled and a new asphalt course was paved on it (shown in Figure 7), which helps to improve driving comfort, increase the antisliding ability, and ensure driving safety. However, the base course inside the tunnel is still directly connected with the pavement outside the tunnel and has the possibility of shear failure.

Table 1: Distress investigation results of Yangkou tunnel.

Detection lane	Stake number	International roughness index (IRI) (m/km)				
		2008	2009	2011	2012	2013
Left (up)	K62 + 000	1.51	1.63	0.99	1.02	1.13
	K61 + 000	1.43	0.99	0.66	0.87	1.03
	K60 + 000	1.59	1.48	0.63	0.96	1.25
	K59 + 000	1.67	1.16	0.57	0.97	1.16
	K58 + 000	2.00	1.27	0.84	1.28	1.48
Right (down)	K57 + 000	2.06	1.74	1.38	1.36	1.42
	K58 + 000	1.79	1.40	0.68	1.03	1.14
	K59 + 000	1.60	1.45	0.85	1.23	1.03
	K60 + 000	1.42	1.21	0.62	0.89	1.14
	K61 + 000	1.39	1.37	0.74	0.90	1.19
Detection lane	Stake number	Rutting depth (mm)				
		2008	2009	2011	2012	2013
Left (up)	K62 + 000	5.0	6.0	4.0	9.0	12.0
	K61 + 000	4.0	7.0	4.0	12.0	11.0
	K60 + 000	5.0	7.0	3.0	13.0	11.0
	K59 + 000	5.0	7.0	4.0	12.0	11.0
	K58 + 000	6.0	6.0	3.0	10.0	11.0
Right (down)	K57 + 000	7.0	5.0	3.0	12.0	15.0
	K58 + 000	5.0	4.0	4.0	10.0	13.0
	K59 + 000	4.0	5.0	3.0	8.0	14.0
	K60 + 000	5.0	5.0	4.0	7.0	14.0
	K61 + 000	5.0	5.0	4.0	11.0	13.0
Detection lane	Stake number	Friction coefficient				
		2008	2009	2011	2012	2013
Left (up)	K62 + 000	69.2	72.0	50.0	62.5	48.6
	K61 + 000	69.6	70.7	53.9	59.7	40.9
	K60 + 000	67.0	65.8	55.5	57.3	44.1
	K59 + 000	59.8	86.9	58.3	57.6	44.1
	K58 + 000	54.6	67.1	53.7	56.6	47.4
Right (down)	K57 + 000	65.6	33.4	74.4	63.6	42.9
	K58 + 000	60.8	33.3	65.2	63.4	47.6
	K59 + 000	61.5	35.6	73.4	61.7	49.4
	K60 + 000	60.8	38.6	77.9	59.7	47.2
	K61 + 000	58.9	34.9	79.7	59.3	42.1

Figure 4: The detection lane areas.

4. Pavement Structure and FE Model

4.1. Pavement Structure. The pavement structure in the entrance and exit sections of the Huangjiayu tunnel is shown in Figure 8 (all acronyms in Figures 8 and 9 are explained in Table 2), and it was referred to as Str-1. A concrete slab is set at the junction part, which can reduce the adverse impact on the

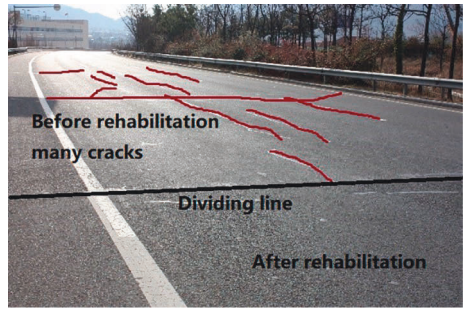

Figure 5: Transverse and longitudinal cracks on the surface of the pavement in the entrance section of the Yangkou tunnel.

Figure 6: The Yangkou tunnel after rehabilitation.

Figure 7: Paving new asphalt course.

structure caused by the large strength gap between the bearing layer and the underlying layer inside and outside the tunnel to a certain extent.

The original pavement structure in the entrance and exit sections of the Yangkou tunnel before rehabilitation is shown in Figure 9, and it was referred to as Str-2. The asphalt pavement outside the tunnel is directly connected with the concrete pavement inside the tunnel without any treatment on load-bearing transition.

4.2. Pavement FE Model. In this study, FE program ANSYS was used. The FE model is shown in Figure 10. The dimensions of the FE model are 4 m × 5 m × (5 m + the length

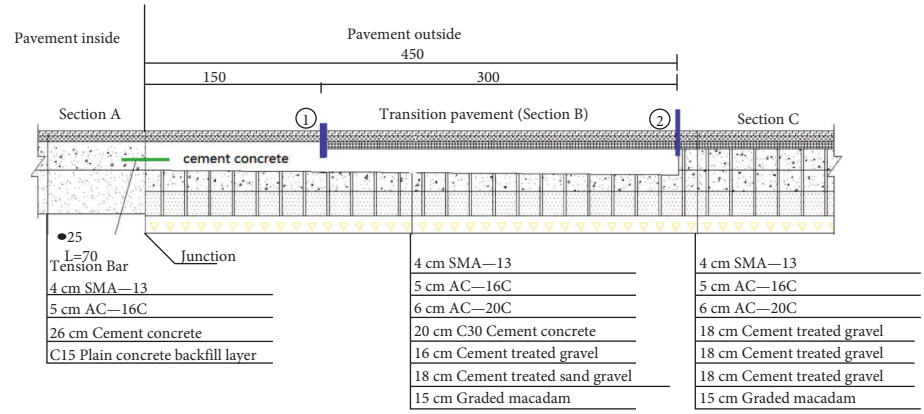

Figure 8: Pavement structures in the entrance and exit sections of the Huangjiayu tunnel (Str-1).

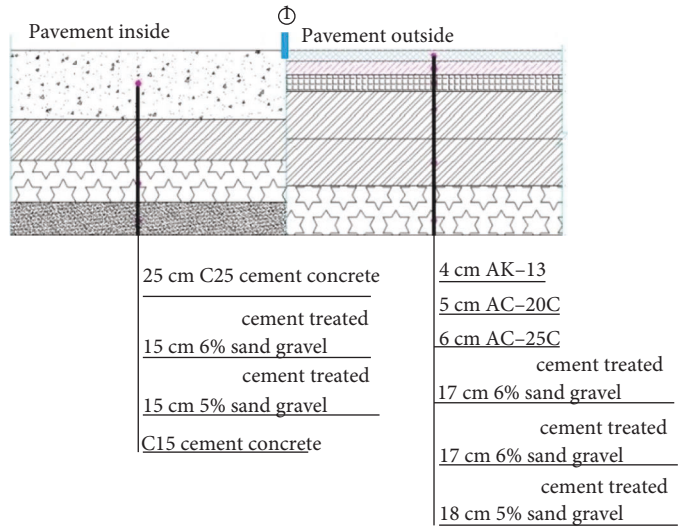

Figure 9: The original pavement structures in the entrance and exit sections of the Yangkou tunnel (Str-2).

Table 2. Explaination of acronyms in Figures 8 and 9.

SMA-13	Stone mastic asphalt, its nominal maximum aggregate size is 13.2 mm.
AC-16C	Asphalt concrete, its nominal maximum aggregate size is 16 mm. C means course and its void ratio is 4%~10%.
AC-20C	Asphalt concrete, its nominal maximum aggregate size is 19.2 mm. C means course and its void ratio is 4%~10%.
AC-25C	Asphalt concrete, its nominal maximum aggregate size is 26.5 mm. C means course and its void ratio is 4%~10%.
AK-13	Asphalt antisliding surface, its nominal maximum aggregate size is 13.2 mm.
C15	Concrete, its standard value of cube compressive strength is 15 MPa.
C30	Concrete, its standard value of cube compressive strength is 30 MPa.

of the transition section + 5 m) ($x \times y \times z$). The direction of transverse is x-direction, and the dimension is 4 m. The direction of the pavement depth is y-direction, and the dimension is 5 m. The direction of traffic is z-direction, and the dimension is (5 m + length of the transition section + 5 m), in which the length of the tunnel pavement (Section A, shown in Figure 8) is 5 m and the length of average pavement (Section C, shown in Figure 8) is 5 m. SOLID 185 was used to simulate asphalt layers and SOLID 65 was used to simulate the concrete layer.

The Tire-Pavement contact area was simplified to rectangle, which is 0.18 m × 0.20 m ($x \times z$). The mesh sizes were different in different areas. In the area where the traffic loads were applied, it was 0.045 m × 0.02 m × 0.05 m ($x \times y \times z$) in the asphalt layer and 0.045 m × 0.05 m × 0.05 m ($x \times y \times z$) in the cement treated layer and concrete layer. It was 0.167 m × 0.13 m × 0.4 m ($x \times y \times z$) in other areas.

4.3. Mechanical Boundary Condition and Traffic Loads. In this paper, Dongfeng EQ-140 was selected as the representative vehicle and its technical parameters are shown in Li's research [23]. The tire load was simplified as the uniformly distributed rectangular load.

4.3.1. Vertical Traffic Loads. In this paper, to simplify the calculation and simulation, traffic loads could be estimated using the haversine function as the following equation [24]:

$$P(t) = P_{\max} \sin\left(\pi \frac{t}{T}\right), \quad (1)$$

$$P_{\max} = \text{PDAF}, \quad (2)$$

where $P_{\max}$ (MPa) is the peak value of the vibrating load, T (s) is the period of traffic loads, t (s) is the time, P (MPa) is the uniformly distributed traffic loads, $P = 0.7$ MPa in China, and DAF is the dynamic amplification factor.

$$\text{DAF} = 1 + a\sqrt{V}, \quad (3)$$

where V (km/h) is the speed; in this study, $V = 60$ and 70 km/h, and a is the riding quality evaluation factor, correlated with IRI, and in this study, $a = 0.035$ [25].

T could be calculated using the following formula:

$$T = \frac{12R}{v}, \quad (4)$$

where R (m) is the equivalent radius of single wheel load, $R = 3L/2$, and L is the length of the uniformly distributed rectangular load; in this study, $L = 0.20$ m, and v (m/s) is the speed. Hence, calculation results of the period of traffic loads (T), the dynamic amplification factor (DAF), and the peak value of the vibrating load ($P_{\max}$) under different traffic speeds are shown in Table 3.

4.3.2. Horizontal Traffic Loads

(1) Longitudinal Friction Stresses. The longitudinal tangential stresses are affected by many factors, such as texture depth of the pavement surface, humidity, driving speed, and textures of tires. According to reference [26], the friction coefficient of the asphalt pavement under different driving speeds was measured through the sideways-force coefficient routine investigation machine (SCRIM), and the relationship between the friction coefficient and the driving speed was shown as follows:

$$\mu = -0.00695\text{V} + 0.87495, \quad (5)$$

where μ is the friction coefficient of the asphalt pavement and V is the driving speed (km/h).

(2) Transverse Tangential Stresses. In addition to the vertical pressure and the longitudinal friction stresses, vehicles would also cause transverse tangential stresses [27], shown in Figure 11.

AL-Qadi et al. [28] measured the three-dimensional contact stress caused by the tire on the pavement and found that the transverse tangential stresses are about 0.183 times of the vertical stresses. Therefore, in this paper, the transverse tangential stress is taken as 0.183 times of the vertical stress.

4.4. Mechanical Parameters. The mechanical parameters are listed in Table 4 [29, 30], based on the Chinese Specifications for Design of Highway Asphalt Pavement (JTG D50-2017). The dynamic modulus of asphalt mixture in Table 4 is that under 20°C and 10 Hz.

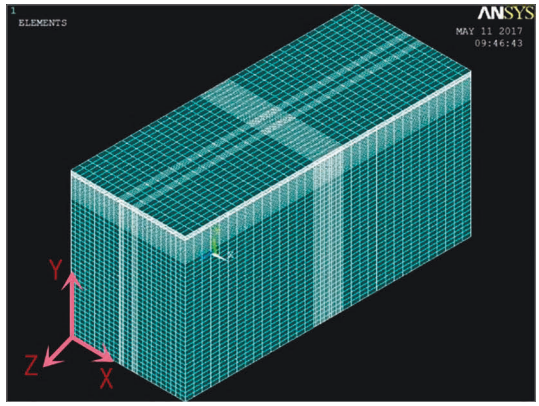

Figure 10: The FE model in this study.

Table 3: Calculation results of T, DAF, and $P_{\max}$ under different traffic speeds.

Speed (km/h)	60	80	100	120
T (s)	0.077	0.058	0.046	0.038
DAF	1.271	1.313	1.350	1.383
$P_{\max}$ (MPa)	0.890	0.919	0.945	0.968

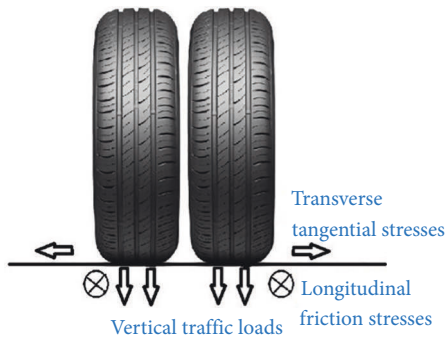

Figure 11: Contact stresses (vertical, transverse, and longitudinal).

4.5. Verification of FE Simulation Results. To verify the finite element simulation results in this paper, taking the pavement in Section C in Str-1 as an example, the mechanical responses calculated by the finite element method and the elastic multilayer theory assumption are compared and analyzed.

The elastic multilayer theory assumption is the standard method in the Chinese Specifications for Design of Highway Asphalt Pavement (JTG D50-2017) to calculate the mechanical responses. It takes the maximum value of Point A, B, C, and D (shown in Figure 12) as the calculation result in this cross section, and the tire load was simplified as the uniformly distributed double circular load.

The calculation results of the tensile strain at the bottom of the asphalt layer along the driving direction and the tensile stress at the bottom of the cement treated layer along

Table 4: Mechanical parameters of pavement materials.

Material	AK-13	SMA-13	AC-16	AC-20	AC-25
Dynamic modulus E^* (MPa)	6800	7000	9000	9500	10000
Poisson's ratio μ	0.25	0.25	0.25	0.25	0.25
Density ρ (kg/m^3)	2400	2400	2450	2480	2505
Material	Cement-treated sand gravel	Graded macadam	Subgrade	C15	C30
Dynamic modulus E^* (MPa)	16000	150	65	20000	30000
Poisson's ratio μ	0.25	0.35	0.40	0.2	0.2
Density ρ(kg/m^3)	2300	2250	1700	2450	2500

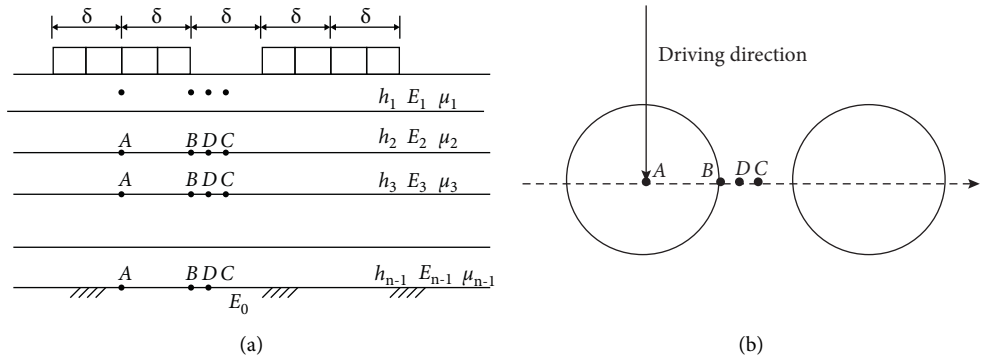

Figure 12: Mechanical response calculation points in the elastic multilayer theory assumption.

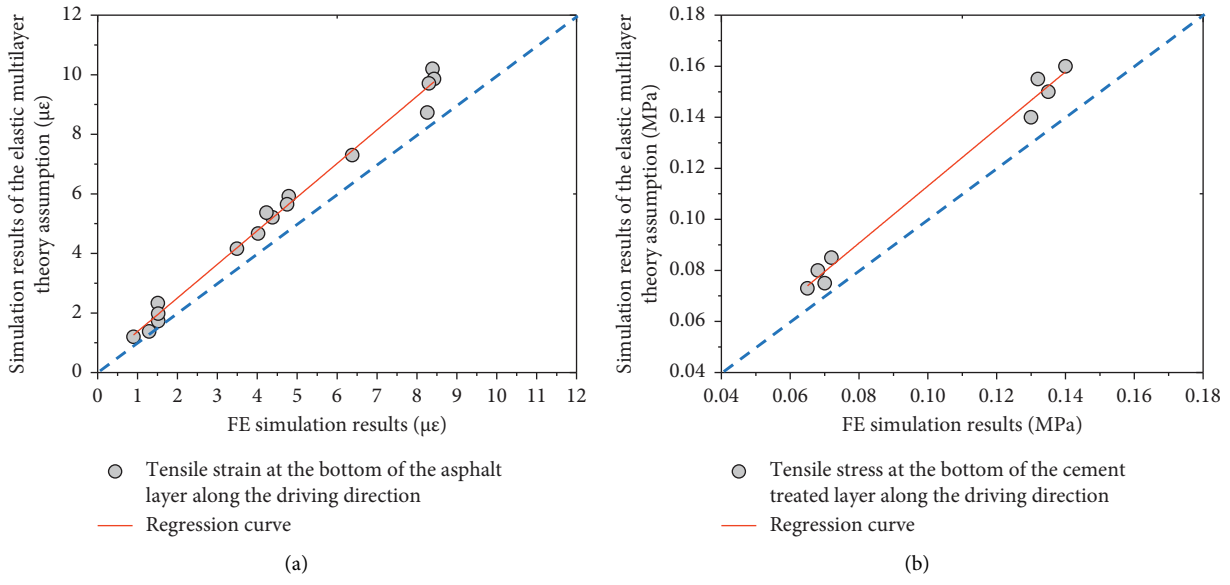

Figure 13: The calculation results of two methods. (a) The calculation results of the tensile strain at the bottom of the asphalt layer along the driving direction. (b) The calculation results of tensile stress at the bottom of the cement treated layer along the driving direction.

the driving direction under the application of the standard axle load BZZ-100(100 kN) are shown in Figure 13.

If the calculation results of the finite element method are completely consistent with the calculation results of the elastic multilayer theory assumption, the calculation results shall be distributed along the dotted line in Figure 13. It can be seen from Figure 13 that although the calculation results of the two methods are not completely consistent, there is a significant linear relationship between them in general, which can be expressed by the followingequations:

$$\text{asphalt layer: EL} = 1.1290 \times \text{FE} + 0.2458\text{R}^2 = 0.9891, \quad (6)$$

$$\text{cement treate d layer: EL} = 1.1182 \times \text{FE} + 0.00125\text{R}^2 = 0.9861, \quad (7)$$

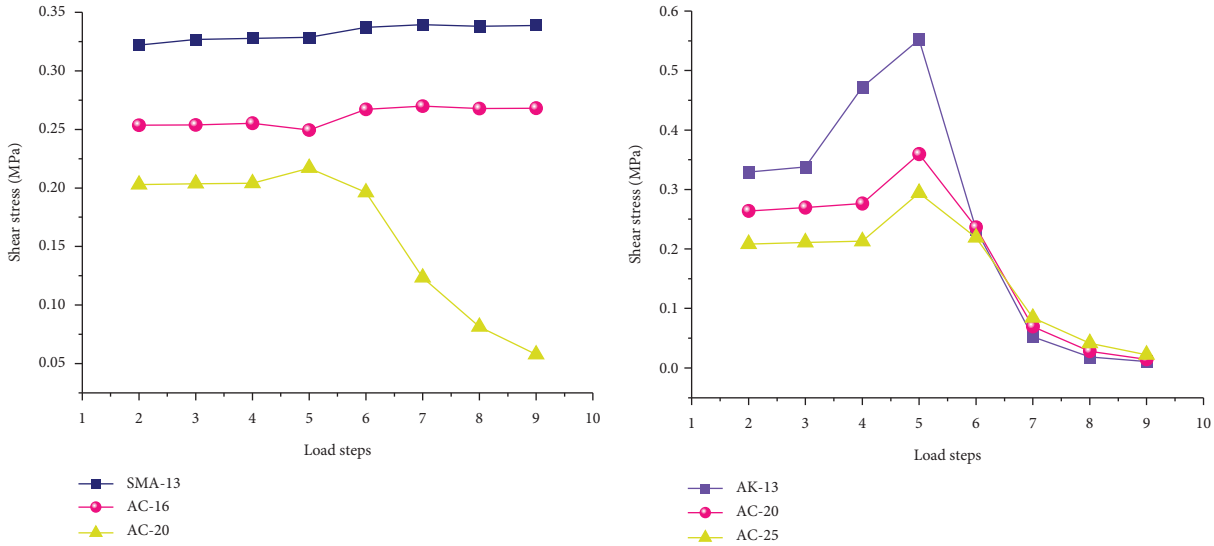

FIGURE 14: Shear stress response of the asphalt pavement outside the tunnel. (a) Maximum shear stress outside tunnel in Str-1. (b) Maximum shear stress outside tunnel in Str-2.

where FE is the calculation results of the finite element method and EL is the calculation results of the elastic multilayer theory assumption.

Therefore, the reliability of finite element calculation results can be guaranteed.

5. Analysis and Discussion of Mechanical Responses of Transition Structure

5.1. Analysis and Discussion of the Influence of Transition Structures. To make a comparison between the mechanical responses of the Yangkou tunnel and the Huangjiayu tunnel, traffic loads of 60 km/h and acceleration of $-0.16\ m/s^2$ [31] were applied, to simulate the process of driving into a tunnel. A transition structure was designed in the junction part in the Huangjiayu tunnel (shown in Figure 8), and there is no transition structure in the entrance and exit sections of the Yangkou tunnel (shown in Figure 9).

In Part 5.1, the necessity of setting a transition section would be analyzed. Moving loads were applied on the structure and the load step 5 was exactly applied on the interfaces, which was Position ① in Str-1 and Str-2 (shown in Figures 8 and 9), respectively. In addition, the simulation result of load step 1 was discarded because there is a large difference between the simulation result of load step 1 and other steps.

5.1.1. Influence of Transition Structure on Asphalt Courses. The discontinuity of the structural layer will have a great impact on the shear performance, and therefore the shear stress response of the asphalt pavement outside the tunnel was firstly analyzed, as shown in Figure 14.

It is shown in Figure 14 clearly that when the loads pass through the transition section, whether to set the transition structure will have a great impact on the mechanical responses of the asphalt pavement in this section. Specifically, there is a significant difference in the shear stress of the asphalt layer between Str-1 and Str-2.

It can be seen from Figure 14(a) that when driving through Position ① of Str-1, the maximum shear stress of asphalt course suddenly changes at load step 5. The shear stresses of the SMA-13 layer and the AC-16 layer almost do not change, while shear stress of the AC-20 layer suddenly decreases. It is possibly when the lower layer of asphalt changes into cement concrete, it would result in poor continuity of pavement structure and sudden change of stress. Besides, in spite of this, the shear stresses of each structural layer are still within the allowable range.

In contrast to Figure 14(b), for load step 5 on Str-2, the asphalt surface layer outside the tunnel is subject to a large stress mutation, which is far more than that of Str-1, which is very unfavorable. Taking the shear stress of the asphalt surface outside the tunnel as an example, the shear stress of the AC-20 layer of Str-1 decreases suddenly, and the variation range of shear stress is 6.43%. For Str-2, not only the shear stresses of the three asphalt layers increase suddenly but also the variation range is huge. The variation range of the AK-13 layer is 16.93% and that of the AC-20 layer and the AC-25 layer is 30.08% and 38.02%, respectively.

In addition, it can be seen from Figure 14 that the shear stresses of the upper layer of the two structures are greater than those of the middle layer. For average highway, the maximum shear stress of the asphalt layer is about 5-6 cm below the road surface, while for tunnel entrances and exits, the maximum value is obtained from the upper layer, which may be due to the high horizontal stress on the pavement surface caused by frequent braking of vehicles, resulting in the upward movement of the position of the maximum shear stress of the asphalt layer.

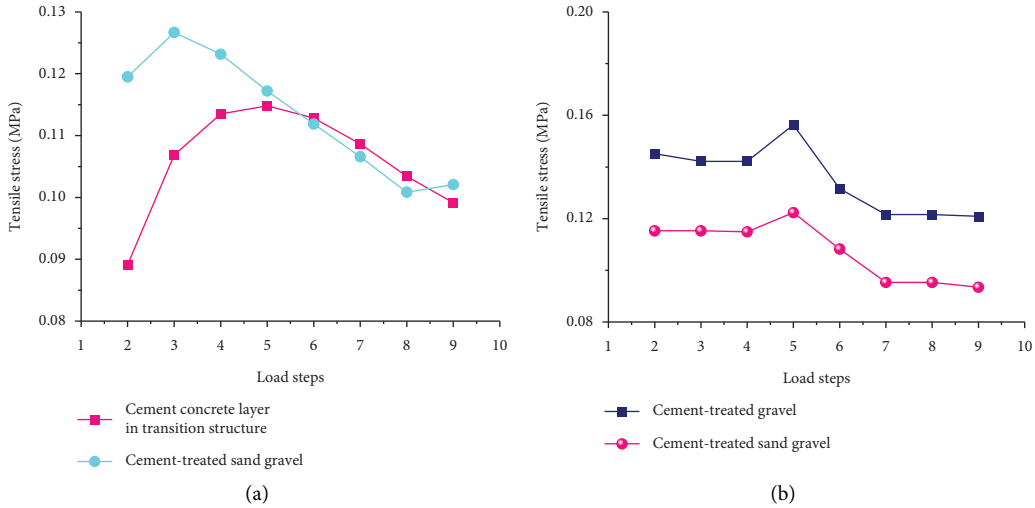

Figure 15: Tensile stress at the bottom of base course outside the tunnel. (a) Tensile stress at the bottom of base course in Str-1. (b) Tensile stress at the bottom of base course in Str-2.

Therefore, based on the above analysis, it is considered that setting transition structure is essential. There are great differences in the pavement structure inside and outside the tunnel. If the structural differentiation design cannot be carried out, the pavement will be damaged prematurely and cause economic losses.

5.1.2. Influence of Transition Structure on Base Course. Tensile stresses at the bottom of the base course outside the tunnel of Str-1 and Str-2 are shown in Figure 15.

It can be seen from Figure 15 that due to the transition structure, there is a significant difference of tensile stress at the bottom of base course outside tunnel between Str-1 and Str-2, in the process of driving through the structural change.

It can be seen from Figure 15(a) that for the cement-treated gravel layer of Str-1, the tensile stress at the bottom of the layer decreases with the load moving forward after load step 3. For the concrete layer in transition structure, the tensile stress at the bottom of base course reaches the peak at load step 5. In addition, the tensile stress at the bottom of the cement-treated gravel layer exceeds that of the concrete layer at first. However, this is reversed afterwards. It is possibly because of the change of base course thickness. With the increase of the thickness of the concrete layer, its bearing proportion increases and gradually exceeds that of the cement-treated gravel layer. Hence, the tensile stress at the bottom changes.

Since the interface of Str-2 is located at the portal, load steps 2~4 were directly applied on the pavement outside the tunnel and load steps 6~9 were applied on the pavement inside the tunnel. To ensure reasonableness of the tensile stress extracted, the tensile stress outside the tunnel was extracted from the bottom of the base course, and the tensile stress at the same depth was extracted for pavement inside the tunnel, as shown in Figure 15(b).

Figure 15(b) shows that in the process of entering the tunnel, the tensile stress will suddenly change at load step 5, and the tensile stress at the bottom of the base course outside the tunnel exceeds that inside the tunnel. It is probably because load step 5 was applied on the interface between pavements inside and outside the tunnel, causing tensile stress at the bottom of the base course increase sharply. At the same time, because the concrete surface layer is used inside the tunnel and its bearing capacity is higher than that of the asphalt surface layer outside the tunnel, the tensile stress at the bottom of the base course in the tunnel is quite small.

Comparing the stress of the base course in Figures 15(a) and 15(b), the maximum tensile stress at the bottom of the upper base course and the lower base course of Str-2 is higher than that of the corresponding structure in Str-1. Therefore, transition structure can significantly improve performance of pavement structure in the entrance and exit sections, which is conducive to the realization of differentiated structure design.

5.1.3. Influence of Overloading. To evaluate the influence of overloading on the mechanical responses of the pavement structure in the entrance and exit sections, the tensile stress at the bottom of the cement treated gravel layer inside and outside the tunnel is analyzed, and the simulation results are shown in Figure 16.

From Figure 16, it is found that the tendency of the maximum tensile stress at the bottom of the base course of Str-1 and Str-2 is same, when the traffic loads increase and move forward. Therefore, with the increase of traffic loads, the stress of pavement structure will become more and more unfavorable. When the standard axle load increases to 20% and 50% overloading, respectively, the maximum tensile stress of Str-1 increases by 20.16% and 47.79%, respectively, while that of Str-2 increases by 23.58% and 51.47%, respectively.

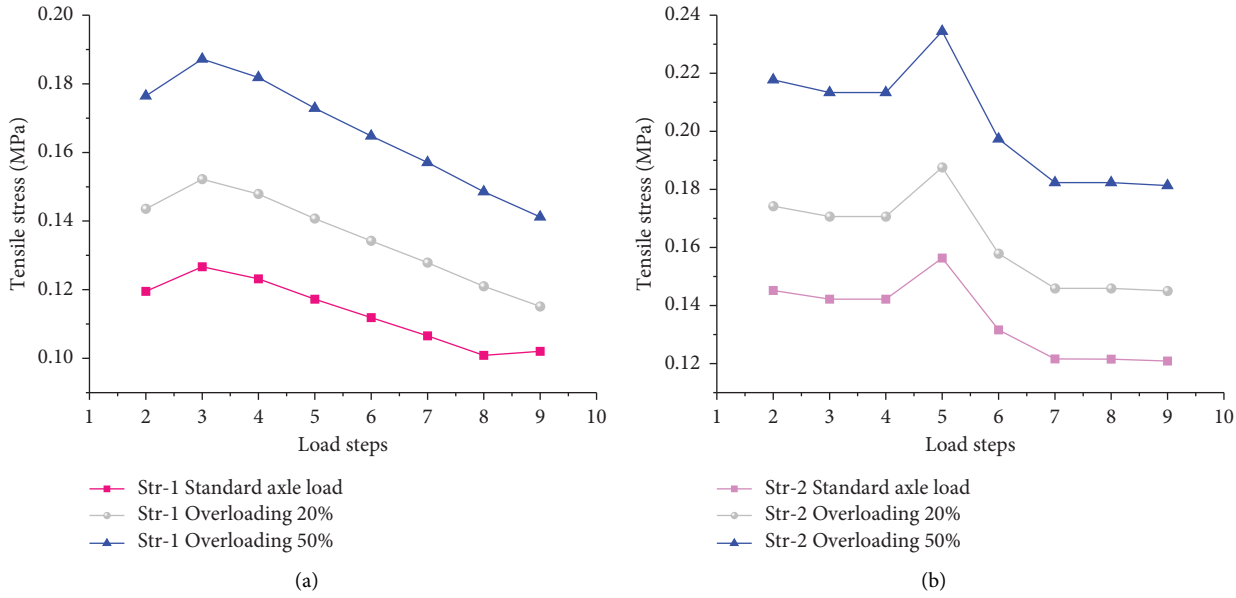

Figure 16: Maximum tensile stress at the bottom of the base course under the application of different overloading. (a) Maximum tensile stress in Str-1. (b) Maximum tensile stress in Str-2.

Based on all the analysis in this section, it is considered that for the asphalt pavement in the entrance and exit sections, ensuring the structural continuity, carrying out differential design, and reasonably setting the transition structure will significantly decrease the stress of the pavement and reduce the probability of cracks and other distresses. Therefore, Str-1 is more reasonable.

5.2. Analysis and Discussion of Transition Structures of Seven Alternative Pavements. Based on the analysis of Part 5.1, Str-1 is superior to Str-2 considering tensile stress at the bottom of the base course and shear stress of the asphalt course. Therefore, in this section, Str-1 will be studied further. First, Str-1 and its 7 alternative pavements were proposed. Then, their mechanical responses under the application of traffic loads were analyzed.

5.2.1. Seven Alternative Pavements. Although Str-1 is superior to Str-2 due to the transition structure, however, this transition part was determined by experience without mechanical simulation, and there are no regulations on transition structure design in the Chinese Specifications for Design of Highway Tunnels (JTG 3370.1-2018) and Chinese Specifications for Design of Highway Asphalt Pavement (JTG D50-2017). Hence, 7 alternative pavements were proposed based on Str-1 and are shown in Figures 17(b)–17(h), and Figure 17(a) shows Str-1, to propose a more reasonable transition structure.

Among them, in Figure 17(b), the asphalt pavement is used both inside and outside the tunnel, which reflects pavement of the Yangkou tunnel after rehabilitation. In Figures 17(c) and 17(d), a concrete slab is inserted into the pavement outside the tunnel and the lower asphalt layer and the upper base course transit into concrete slab simultaneously. The length of the concrete slab is 4.5 m and 6 m, respectively. In Figures 17(e)–17(h), the inserted concrete slab has variable cross section. Also, the cross section of inserted concrete slab in Str-1 is variable. The length of the concrete slab in Figures 17(e) and Figures 17(f) and 17(h) is 4.5 m and 6 m, respectively.

In addition, according to the Chinese specifications, the length of the pavement concrete slab shall not exceed 6 m and 4~6 m should be adopted. Therefore, the length of the concrete slab in the pavement structures shown in Figure 17 is set to be 4.5 m and 6 m, respectively.

5.2.2. Analysis and Discussion. 9 load steps of 70 km/h and $-0.16\ m/s^2$ were applied. The load step 5 was exactly applied on the marking place of 8 pavements, and the marking place is shown in Figures 17(a)–17(h) in blue. The simulation results are shown in Table 5.

From Table 5, it can be found that compared with Str-1a, Str-1 and Str-1b~ Str-1g with transition structure can significantly reduce the maximum shear stress in the asphalt course inside and outside the tunnel. Therefore, concrete slab at the connection part can effectively help pavement transition.

It is also shown that compared with Str-1b and Str-1c, when the length of a concrete slab is 4.5 m (Str-1b), the shear stress of each layer is relatively small. Therefore, when the lower asphalt layer and the upper base course transit into the concrete slab simultaneously, it is more reasonable to set the concrete slab at 4.5 m. It can also be understood that when the asphalt surface inside and outside the tunnel is designed to be two layers, it is more reasonable to use Str-1b.

To make a comparison among Str-1and Str-1d~Str-1g and determine the reasonable length of the concrete slab, simulation results when traffic loads were applied on position ② are extracted and shown in Figure 18.

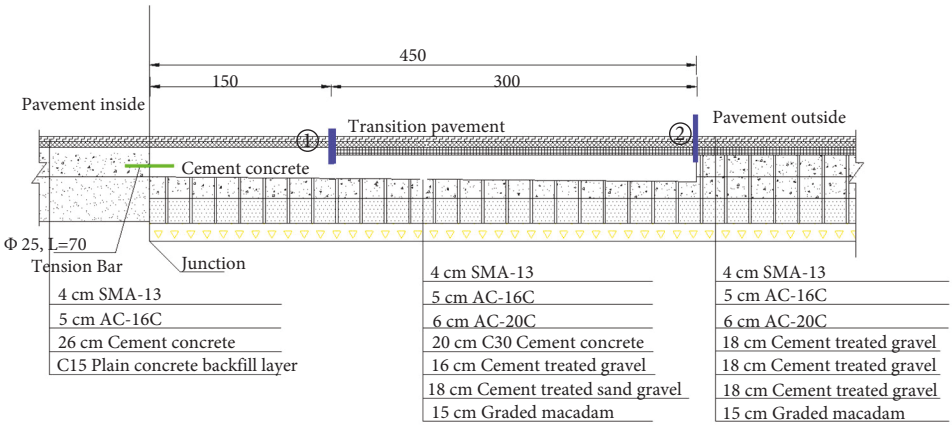

(a)

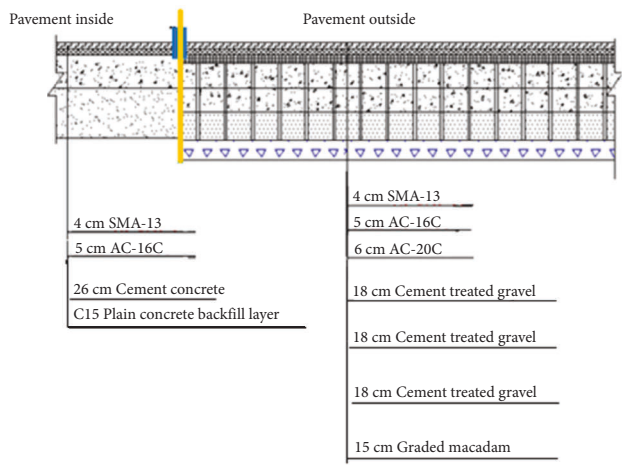

(b)

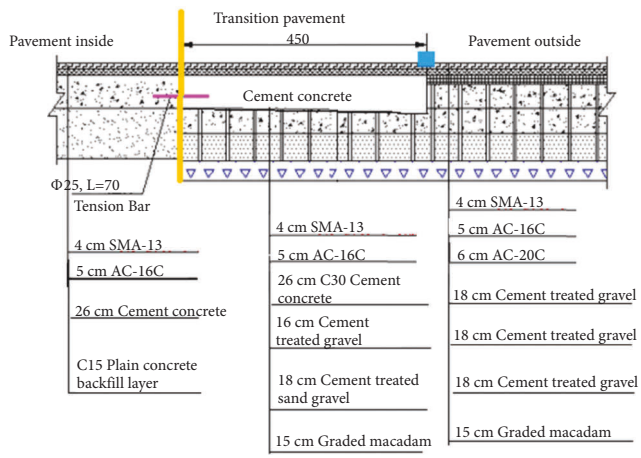

(c)

Figure 17: Continued.

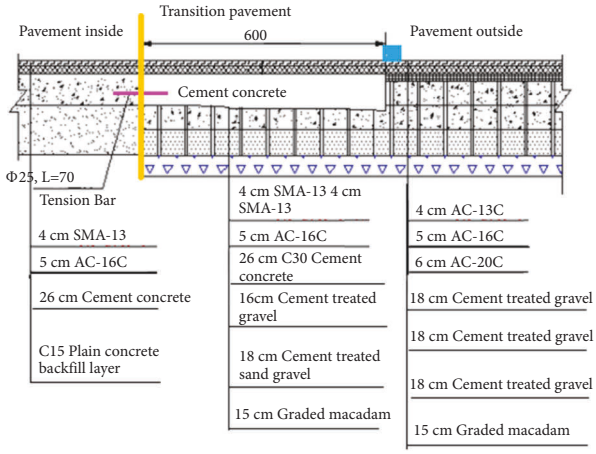

(d)

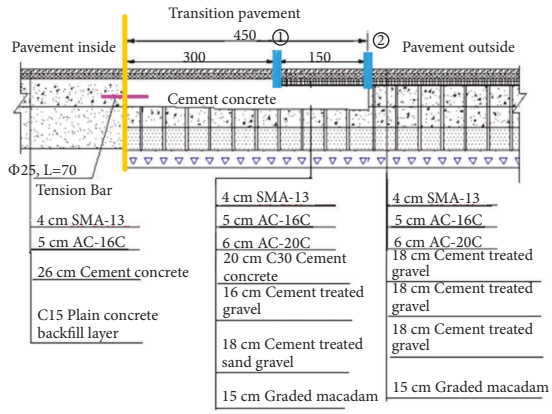

(e)

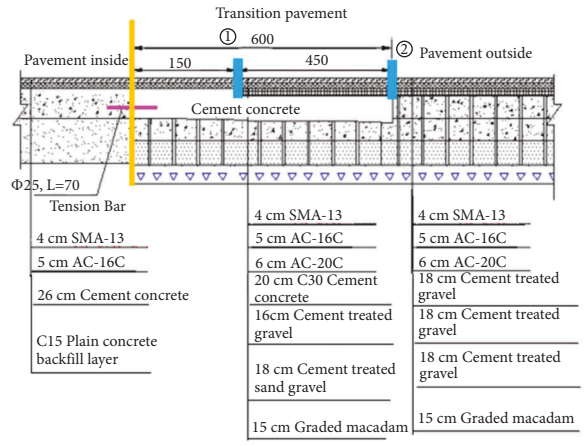

(f)

Figure 17: Continued.

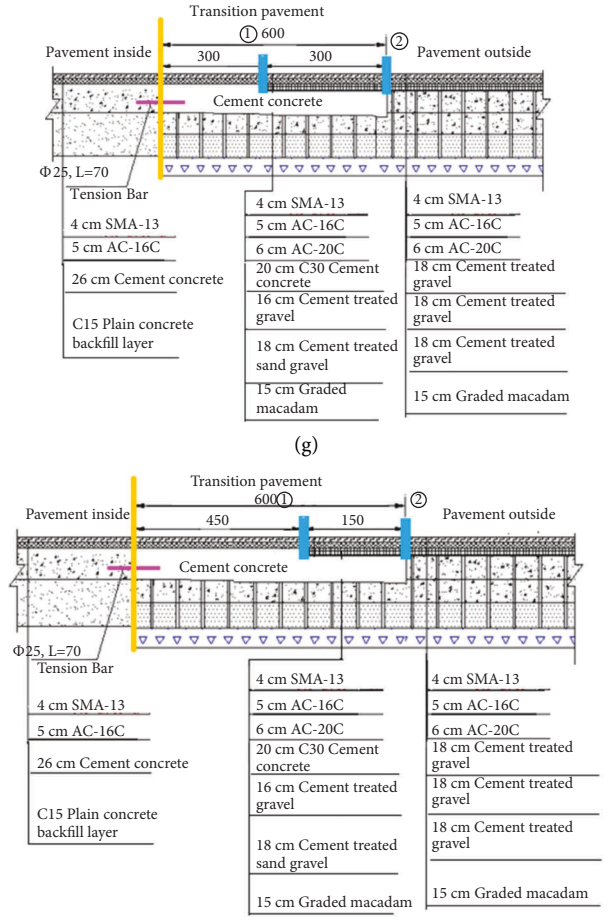

Figure 17: Str-1 and 7 alternative pavement structures. (a) Str-1. (b) Str-1a. (c) Str-1b. (d) Str-1c. (e) Str-1d. (f) Str-1e. (g) Str-1f. (h) Str-1g.

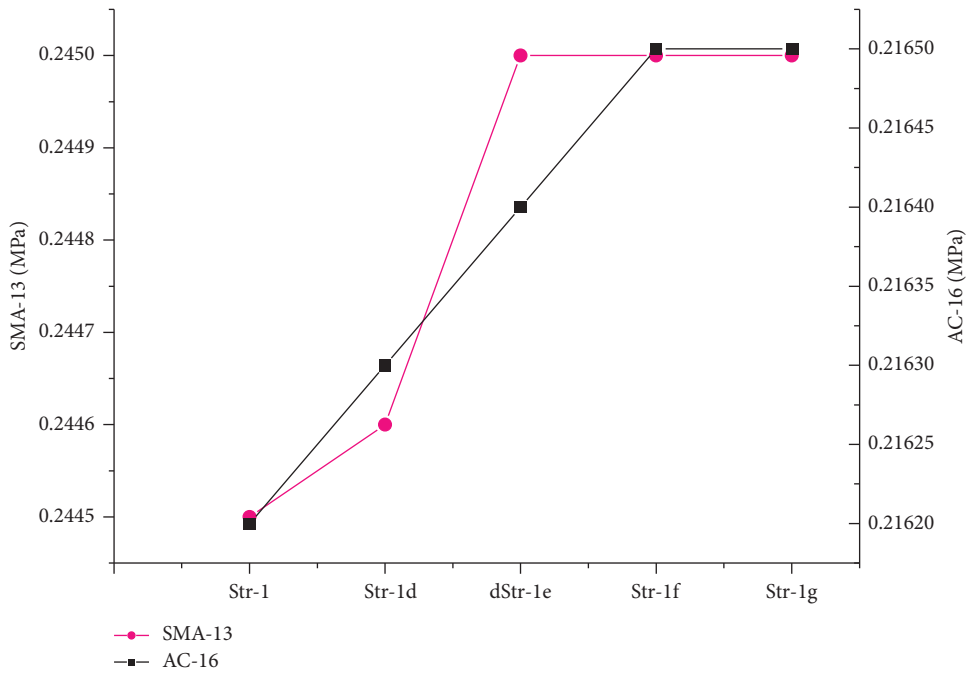

(a)

Figure 18: Continued.

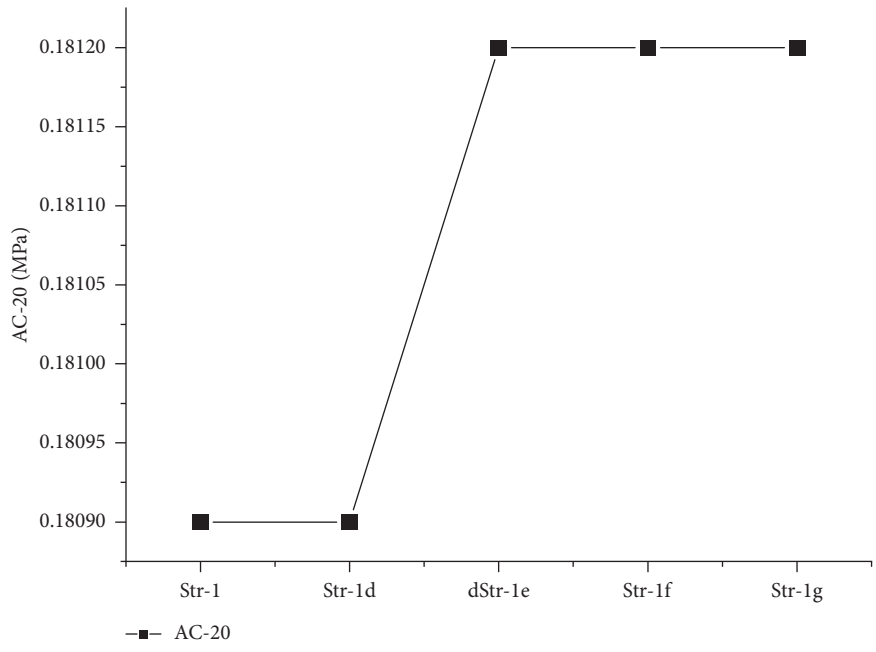

(b)

Figure 18: Maximum shear stress in the asphalt course of Str-1and Str-1d~Str-1g. (a) Maximum shear stress in the upper and middle asphalt layers. (b) Maximum shear stress in the lower asphalt layer.

Table 5: Simulation results of 8 pavement structures under the application of traffic loads (MPa).

Structure	Marking place	Pavement outside					Pavement inside		
		Maximum shear stress in asphalt course			Tensile stress at the bottom of base course		Maximum shear stress in asphalt course		Tensile stress at the bottom of base course
		SMA-13	AC-16	AC-20	Concrete slab	Cement treated gravel	SMA-13	AC-16	Concrete pavement
Str-1	①	0.2516	0.2191	0.2064	0.0288	0.0680	0.0253	0.0443	0.1203
	②	0.2445	0.2162	0.1809	0.0198	0.0974	0.0170	0.0319	0.0883
Str-1a	—	0.2658	0.2299	0.2343	—	0.0235	0.2443	0.2185	0.0697
Str-1b	—	0.2447	0.2132	0.2051	0.0806	0.0966	0.0171	0.0323	0.0894
Str-1c	—	0.2451	0.2134	0.2056	0.0464	0.0933	0.0087	0.0170	0.0477
Str-1d	①	0.2471	0.2166	0.2009	0.0256	0.0916	0.0241	0.0441	0.1304
	②	0.2446	0.2163	0.1809	0.0199	0.0973	0.0172	0.0324	0.0961
Str-1e	①	0.2515	0.2190	0.2063	0.0288	0.0683	0.0250	0.0437	0.1288
	②	0.2450	0.2164	0.1812	0.0177	0.0944	0.0082	0.0162	0.0482
Str-1f	①	0.2472	0.2166	0.2010	0.0253	0.0911	0.02359	0.0430	0.1274
	②	0.2450	0.2165	0.1812	0.0178	0.0943	0.0085	0.0167	0.0498
Str-1g	①	0.2467	0.2164	0.2002	0.0233	0.0936	0.0166	0.0312	0.0925
	②	0.2450	0.2165	0.1812	0.0179	0.0941	0.0086	0.0169	0.0503

Note. The tensile stress at the bottom of the base course in Table 5 takes the larger value of the tensile stress along the driving direction and perpendicular to the driving direction.

It can be seen from Figure 18 that the maximum shear stress in asphalt surface outside the tunnel increases with the increase of the length of a concrete slab. When the length of a concrete slab is 4.5 m (Str-1 and Str-1d), the maximum shear stress in the surface is the lowest. Therefore, it can be preliminarily concluded that whether the lower asphalt layer and the upper base course transit into concrete slab simultaneously or not, when the length of the concrete slab is 4.5 m, the maximum shear stress in the asphalt layer of the pavement outside the tunnel is the lowest, which may be due to the fact that when the concrete slab is longer (>4.5 m), it exceeds the appropriate length, making the pavement outside the tunnel indirectly become the asphalt pavement with rigid base, resulting in the increase of the maximum shear stress in the asphalt layer.

Since the length of the concrete slab set in Str-1, Str-1b, and Str-1d is 4.5 m, therefore the three pavement structures are further compared. Firstly, Str-1 and Str-1d are compared.

Since the stress has been analyzed when the moving loads were applied at position ②, the stress when the moving loads were applied at position ① would be analyzed in this part. When the moving load was applied on position ①, the maximum shear stress in the asphalt layer and the tensile stress at the bottom of the base course of Str-1 are less than those of Str-1d (shown in Table 4). Hence, Str-1 is better. It can also be understood that when the asphalt surface outside the tunnel is designed to be three layers and the asphalt surface inside the tunnel is designed to be two layers, the Str-1 is more reasonable.

To sum up, it can be concluded that when the asphalt surface outside the tunnel is designed to be three layers, it is more appropriate to use Str-1 as the tunnel transition pavement. When the asphalt surface outside the tunnel is designed to be two layers, Str-1b is more reasonable.

6. Conclusion

The entrance and exit sections of a tunnel are subject to different environments, pavements, and traffic conditions, which is quite different from the ordinary highway section, and it should be considered differentially, when designing the pavement structures. Although a lot of studies were carried on the entrance and exit sections of a tunnel, there are few ones on the mechanical response characteristics of the pavement structures. In this paper, the Huangjiayu tunnel of Qingdao-Lanzhou Highway and the Yangkou tunnel of Qingdao Binhai Highway in Shandong province were taken as case study engineering. Meanwhile, 7 other alternative pavement structures were proposed, simulated, and analyzed through ANSYS. It can be concluded that

(1) Setting transition structure is essential and it can ensure the continuity of the pavement and significantly reduce the sudden change of shear stress of the asphalt layer and thus prevent premature pavement damaged.

(2) For the asphalt pavement in the entrance and exit sections, ensuring the structural continuity, carrying out differential design, and reasonably setting the transition structure will significantly decrease the stress of the pavement and reduce the probability of cracks and other distresses. Hence, Str-1 is more reasonable compared with Str-2.

(3) As Yangkou tunnel, even if the concrete course was milled and an asphalt course was paved, its pavement structure is still quite different from that of Str-1 in the structural continuity. Hence, it is recommended that when a pavement structure like this was rehabilitated, applying a transition structure would be necessary.

(4) When the asphalt course outside the tunnel is designed to be three layers, it is more appropriate to use Str-1 as the tunnel transition pavement, whose concrete slab has variable cross section, and the length of the concrete slab is 4.5 m. When the asphalt surface outside the tunnel is designed to be two layers, Str-1b is more reasonable and the length of the concrete slab is also 4.5 m.

Data Availability

The data that support the findings of this study are available from the corresponding author upon reasonable request.

Disclosure

Research prospect: in future, authors would make an investigation to distresses of the pavement structures in the sections of tunnel entrances and exits, especially the Yangkou tunnel and Huangjiayu tunnel.

Conflicts of Interest

The authors declare that there are no conflicts of interest.

Acknowledgments

This research was supported by the Department of Transport of Shandong Province and Shandong Provincial Communications Planning and Design Institute Group Co., Ltd.

References

[1] S. Li, "Temperature field analysis of typical pavement structure at the entrance and exit of tunnel," *Journal of Highway and Transportation Research and Development*, no. 8, p. 4, 2013.

[2] F. Cheng, *Research on the Temperature Field of Alatan Tunnel in Lu-Huo Highway*, Chang'an University, Xi'an, 2009.

[3] Y. Wang, *Research On Pavement Temperature Field At Entrance And Exit Section Of Highway Tunnel In Qinling Mountains 2012*, Chang'an University, Xi'an, 2021.

[4] W. Ji, "research on curve coordination of tunnel inlets and outlets," *Technology of Highway and Transport*, no. 5, p. 3, 2014.

[5] Y. Wang, "Alignment design at tunnel entrance and exit zone based on operating safety," *Journal of Highway and Transportation Research and Development*, vol. 25, no. 3, p. 5, 2008.

[6] Y. Yan, Y. Zhang, and Z. Guo, "Alignment safety evaluation at tunnel entrance and exit based on driving speed," *Journal of Chang'an University(Natural Science Edition)*, vol. 30, no. 4, p. 5, 2020.

[7] Z. Yang, Y. Tang, and L. Tang, "Consistency of horizontal alignment at tunnel entrance and exit zone," *Journal of Tongji University*, vol. 40, no. 4, p. 4, 2012.

[8] H. Bai, "Locating speed limit signs for freeway tunnel entrance and exit," in *Proceedings of the American-Society-of-Civil-Engineers (ASCE) International Conference on Transportation and Development (ICTD)*, Pittsburgh, PA, 2018.

[9] C. Yang, "Research on the lighting of entrance and exit segments of city tunnels and outside-tunnel roads with visual efficiency theory," in *Proceedings of the Conference of the International-Commission-On-Illumination on Lighting Quality and Energy Efficiency*, Hangzhou, PEOPLES R CHINA, 2012.

[10] S. Fu, *Based on the Physiological Characteristics of the Driver the Tunnel Entrance Lighting Research*, p. 58, Chongqing Jiaotong University, Chongqing, 2016.

[11] Y. Li and G. Cheng, "Reasonable length of glare proof grille section at exit and entrance of highway tunnel," *Highway Engineer*, vol. 34, no. 5, p. 4, 2009.

[12] Q. Wang, *Research of Highway Tunnel Entrance and Exit Lignting Configuration Opimization and Control System*, p. 66, Xi'an University of Architecture and Technology, Xi'an, 2014.

[13] G. Zhou, L. J. Li, Q. S. Shi, Y. S. Ouyang, Y. B. Chen, and W. F. Hu, "Efficacy of metal ions and isothiazolones in inhibiting *Enterobacter cloacae* BF-17 biofilm formation," *Canadian Journal of Microbiology*, vol. 60, no. 1, pp. 5–14, 2014.

[14] J. L. Xu, X. Zhang, H. Liu et al., "Physiological indices and driving performance of drivers at tunnel entrances and exits: a simulated driving study," *PLoS One*, vol. 15, no. 12, p. e0243931, 2020.

[15] H. Ma and J. L. Xu, "Iop. The," *Speed Limit Determination of Tunnel Entrance And Exit Section On Rainy Days*, in *Proceedings of the 2nd International Conference on Civil Engineering, Environment Resources and Energy Materials*, Changsha, PEOPLES R CHINA, August 2020.

[16] T. Zhu, C. Wang, C. Yang, and R. Zhao, "Evaluation of effectiveness of speed reduction markings on driving speed in highway tunnel entrance and exit areas," *Promet - Traffic&Transportation*, vol. 32, no. 1, pp. 141–152, 2020.

[17] S. S. Wang, Z. Du, F. Jiao, H. Zheng, and Y. Ni, "Drivers' visual load at different time periods in entrance and exit zones of extra-long tunnel," *Traffic Injury Prevention*, vol. 21, no. 8, pp. 539–544, 2020.

[18] F. Shao, "Measuring safety for urban tunnel entrance and exit based on nanoscopic driving behaviors," in *Proceedings of the 8th International Conference on Measuring Technology and Mechatronics Automation (ICMTMA)*, Macau, PEOPLES R CHINA, October 2016.

[19] X. Zhao, A. Shen, and C. Xue, "Dynamic response of asphalt pavement in tunnel entrance and exit area based on mixture viscoelasticity," *International Symposium on Material, Energy and Environment Engineering*, 2015.

[20] M. AG, "Chinese national administration of surveying,".

[21] H. Wang, "Analysis of traffic accident characteristics in highway tunnel environment," *Highways*, no. 11, p. 4, 2009.

[22] J. Gao, *Research on Pavement Structures and Materials in Import and export of Highway Tunnel Based on the Safety*, p. 80, Chang'an University, Xi'an, 2012.

[23] L. Li, *Research on rutting in the section of steep longitudinal slope ofMountainous Expressway*, Southeast University, Dhaka, Bangladesh, 2013.

[24] Z. Zheng, *Study on Adaptability of Fiber Reinforced Chip Seal in Hot-Moist Region of south China*, Chang'an University, Xi'an, 2013.

[25] L. Huang and C. Sheng, "Relationship between vehicle dynamic amplification factor and pavement roughness," *Journal of Highway and Transportation Research and Development*, no. 03, pp. 27–30, 2006.

[26] Z. Zheng, *Study On Adaptability Of Fiber Reinforced Chip Seal In Hot-Moist Region Of South China 2013*, Chang'an University, Xi'an, 2013.

[27] H. Wang and I. L. Al-Qadi, "Combined Effect of Moving Wheel Loading and Three-Dimensional Contact Stresses on Perpetual Pavement Responses," *Transportation Research Record: Journal of the Transportation Research Board*, vol. 2095, no. 1, pp. 53–61, 2095.

[28] I. L. Al-Qadi, M. Elseifi, and P. J. Yoo, *PAVEMENT DAMAGE DUE TO DIFFERENT TIRES AND VEHICLE CONFIGURATIONS 2004*, pp. 23–55, Virginia Tech Transportation Institute, Blacksburg, 2004.

[29] X. Zhao, A. Shen, and B. Ma, "Temperature response of asphalt pavement to low temperatures and large temperature differences," *International Journal of Pavement Engineering*, vol. 21, no. 1, pp. 49–62, 2018.

[30] X. Y. Zhao, A. Q. Shen, and B. F. Ma, "Temperature adaptability of asphalt pavement to high temperatures and significant temperature differences," *Advances in Materials Science and Engineering*, vol. 2018, pp. 1–16, 2018.

[31] Y. Ma, L. Kong, and Z. Guo, "Safe operating speed and control measure based on lighting transition to tunnel entrance," *Journal of Shandong Jiaotong University*, vol. 15, no. 1, pp. 79–84, 2007.